

Diffractive excitation of 14.6-, 60-, and 200-GeV/nucleon ^{16}O and 14.6-GeV/nucleon ^{28}Si nuclei in nuclear emulsion

S. Y. Bahk,⁽¹²⁾ S. D. Chang,⁽⁷⁾ B. G. Cheon,⁽⁷⁾ J. H. Cho,⁽⁷⁾ H. I. Jang,⁽²⁾ C. H. Hahn,⁽¹⁾
T. Hara,⁽⁶⁾ G. Y. Lim,⁽⁷⁾ J. S. Kang,⁽⁷⁾ C. O. Kim,^(7,9) J. Y. Kim,⁽²⁾ K. Y. Kim,⁽⁷⁾ S. N. Kim,⁽⁸⁾
T. I. Kim,⁽²⁾ T. Y. Kim,⁽⁷⁾ D. G. Koo,⁽¹⁰⁾ S. B. Lee,⁽⁷⁾ I. T. Lim,⁽⁷⁾ K. H. Moon,⁽⁹⁾ S. W. Nam,⁽⁷⁾
M. Y. Pac,⁽²⁾ I. G. Park,^(4,9) J. N. Park,⁽¹¹⁾ J. Y. Ryu,⁽³⁾ T. S. Shin,⁽⁷⁾ K. S. Sim,⁽⁷⁾ J. S. Song,⁽⁴⁾
J. K. Woo,⁽⁷⁾ C. Yokoyama,⁽⁵⁾ and C. S. Yoon⁽⁴⁾

⁽¹⁾*Department of Physic, Changwon National College, Changwon 641-240, Korea*

⁽²⁾*Department of Physics, Chonnam National University, Kwangju 500-757, Korea*

⁽³⁾*Department of Physics, Gunsan National University, Gunsan 573-360, Korea*

⁽⁴⁾*Gyeongsang National University, Jinju 660-300, Korea*

⁽⁵⁾*Department of Physics, Kobe University, Rokkodai-cho, Nada-ku, Kobe 657, Japan*

⁽⁶⁾*College of Liberal Arts, Kobe University, Tsurukabuto, Nada-ku, Kobe 657, Japan*

⁽⁷⁾*Department of Physics, Korea University, Seoul 136-701, Korea*

⁽⁸⁾*Department of Physics, Korea National University of Education, Cheongju 363-890, Korea*

⁽⁹⁾*Department of Physics and Astronomy, Louisiana State University, Baton Rouge, Louisiana 70803*

⁽¹⁰⁾*Seoul National Teacher's College, Seoul 137-742, Korea*

⁽¹¹⁾*Department of Computer Science, Sookmyeong Women's University, Seoul 140-132, Korea*

⁽¹²⁾*Department of Physics Education, Wonkwang University, Iri 570-749, Korea*

(Received 21 May 1990)

An angular method of identifying diffractive excitation (DE) events for interactions of a hadron beam in nuclear emulsion is applied to identifying DE events in interactions of heavy ions beams. The "apparent" mean free paths (MFP) of DE processes for ^{16}O (^{28}Si) beams are 1.00 ± 0.12 , $2.4^{+1.6}_{-0.7}$, and 2.2 ± 0.4 (1.5 ± 0.2) m, respectively, at 200, 60 and 14.6 GeV/nucleon, which corresponds to 20–10 % of the MFP for total inelastic interactions. Distinctive features of diffractively excited nuclei are discussed.

I. INTRODUCTION

A new improved experimental method of identifying diffractive excitation (DE) of projectile *protons* of the primary beam energy $E_b = 30, 200, 300,$ and 400 GeV in nuclear emulsion was introduced by Kim, Hong, and Park in 1980 (see Appendix A),¹ and yielded the reasonable values of mean-free path (MFP) consistent with the conventional $\sum_i \sin\theta_i$ method.² The techniques, which are based on the same principles mainly applied to low-multiplicity events, commonly involve accurate measurement of the emission angles θ (up to 10^{-4} radians) in the laboratory system (LS), and potential DE events are those interactions showing *no visible target excitation* ($N_h = 0$),³ when the interactions are examined in the emulsion using the optical microscopes. Besides its great advantage of studying DE interactions in a wide range of primary beam energies with identical criteria, the angular method of Ref. 1 has been proved to be powerful and easily applicable also for identifying DE events of projectile *heavy ions* of primary beam energies $E_b = 14.6, 60,$ and 200 GeV/nucleon, which is the very subject we report in this paper.

Small- p_T multiparticle production at high energy can be categorized roughly into multiperipheral particle production and DE to higher-mass states, where, in the latter, the nucleus (or excited hadron) subsequently de-

cays into several fragmented nuclei or final-state hadrons.^{4–7} At sufficiently high energy, valid in most of our present cases, the condition of identifying DE events becomes $q_L R \ll 1$, which is that of the "virtuality (or coherence)" with respect to the individual constituents of b ,^{6,7} where q_L is the longitudinal component of the momentum transferred to the target nucleus, and the "interaction" nuclear radius for the projectile heavy ion of mass number A_b and target nucleus of mass number A_t is $R = (A_b^{1/3} + A_t^{1/3})/m_\pi$, m_π being the rest energy of a pion. (Here, the natural unit of $\hbar = c = 1$ is used; $1/m_\pi = 1.45$ fm.) For the projectile nucleus of ^{16}O (^{28}Si), $q_L < 0.040$ (0.035), 0.029 (0.026), and 0.20 (0.018) GeV/c, respectively, for the composite targets of the hydrogen nuclei (H), the light nuclei (C, N, and O), and the heavy nuclei (Ag, Br) in nuclear emulsion.

For the incident heavy ion with an LS primary energy $E_b = m_b \cosh y_b$ in the DE interaction of $b + A_t \rightarrow b^* + A_t$, it is straightforward to derive the good approximate expression for m_{b^*} from energy-momentum conservation. As shown in Appendix A,

$$m_{b^*} \simeq m_b (1 - q_L^2/m_b^2 + 2q_L \sinh y_b/m_b)^{1/2} \quad (1)$$

since the LS energy of b^* ,

$$E_{b^*} = m_{Tb^*} \cosh y_{b^*} \\ = (m_{b^*}^2 + q_T^2)^{1/2} \cosh y_{b^*} \sim m_{b^*} \cosh y_{b^*}$$

(q_T^2 is extremely small), and the energy transferred from the projectile to the target in the DE process, $\Delta E = E_b - E_{b^*}$ ($\simeq q^2/2A, m_N < 0.001$ GeV, m_N being the rest energy of a nucleon) is also negligible. From Eq. (1) for $q_{L\max} = 0.029$ GeV/c, the values $m_b^*/m_b = 1.03, 1.12,$ and 1.36 and $\Delta m = m_{b^*} - m_b = 0.447, 1.764,$ and 5.289 GeV/c², respectively, for 14.6-, 60-, and 200-GeV/nucleon ¹⁶O. For $q_{L\max} = 0.026$ GeV/c, $m_b^*/m_b = 1.0155$ and $\Delta m = 0.404$ GeV/c² for 14.6-GeV/nucleon ²⁸Si.

Because $\Delta E < 0.001$ GeV in the DE process, the *formation time* of b^* should be as long as 10^{-21} sec, i.e., b^* is a sharp resonant state in the continuum above the ground state b (b^* decays long after passing through the target nucleus).⁸ Also, the average of LS rapidities $\langle y \rangle$ of its decay particles in the decay process, $b^* \rightarrow N_1 + N_2 + \dots + \pi + \pi + \dots$, should be y_{b^*} ($= y_b - \Delta y$), where $\Delta y \simeq \ln(m_{b^*}/m_b)$, i.e.,

$$\langle y \rangle = \langle \bar{y} + y_{b^*} \rangle \simeq y_{b^*}, \quad (2)$$

where \bar{y} is the rapidity in the rest frame of b^* and $\langle \bar{y} \rangle \sim 0$, which essentially comes from the requirement of energy-momentum conservation in the rest system of b^* , as stated in detail in Ref. 1, and we would like to assume separately for singly charged or α fragments in the present experiment. This crucial condition has been proved to be largely valid from our data, as shown later. For $q_{L\max} = 0.029$ (0.026) GeV/c, $\Delta y = 0.03$ (0.0155), 0.113, and 0.307, for ¹⁶O (²⁸Si) of $E_b = 14.6, 60,$ and 200 GeV/nucleon, respectively.

For relativistic heavy ion projectiles with E_b up to 200 GeV/nucleon the process called "electromagnetic dissociation or spallation" has been recently reported⁹ to confirm the very existence of the DE process. Furthermore, ¹⁶O events of the same DE interactions as in our present experiment were reported by Ardito *et al.*^{10,11}

In Sec. II, experimental materials and methods are explained. In Sec. III, experimental results are presented, and finally discussions and conclusions are described in Sec. IV.

II. EXPERIMENTAL MATERIALS AND METHODS

Stacks of BR-2 (Fuji ET-7B) emulsion pellicles with dimensions 5×10 cm² \times 600 μ m were exposed horizontally at Brookhaven National Laboratory (BNL) to the 14.6-GeV/nucleon ¹⁶O (²⁸Si) beam and at CERN to 60 and 200-GeV/nucleon ¹⁶O beams. The emulsions were scanned with typical magnification of $500 \times$ by the along-the-track scanning method. However, most of the 14.6-GeV/nucleon ¹⁶O data and all of the ²⁸Si data were obtained using magnifications of $125 \times$ and $750 \times$, respectively. In tracing 69.31, 72.37, and 67.24 m, for 200-, 60-, and 14.6-GeV/nucleon ¹⁶O tracks, respectively, 659 (among them, 187 of $N_h = 0$), 636 (134), and 532 (62) interactions were found and yielded MFP's of 0.105 ± 0.004

m (1.19 ± 0.05 b),¹² 0.114 ± 0.005 m (1.09 ± 0.04 b), and 0.126 ± 0.005 m (0.99 ± 0.04 b), respectively. While in tracing 71.69 m for 14.6-GeV/nucleon ²⁸Si tracks, 737 (137) interactions were found and gave an MFP of 0.097 ± 0.004 m (1.28 ± 0.04 b). Main experimental results about "central collisions" using the ¹⁶O part of the present material have been already reported.¹³

Identification of DE events of *soft splitting* of nuclei, such as ¹⁶O* $\rightarrow 4\alpha$, $\alpha + ^{12}\text{C}$, $p + ^{15}\text{N}$, $2d + ^{12}\text{C}$, and ²⁸Si* $\rightarrow ^{24}\text{Mg} + \alpha$, ²⁷Al + p , etc. is routinely achieved by inspection under the microscope only, and the gross features of their decays can be well understood under the premise of Eq. (2). While the average LS rapidity $\langle y \rangle$ of the decay particles of b^* is y_{b^*} ($\simeq y_b$), that of shower particles of non-DE events is nearly $y_b/2$.

Nevertheless, in the practical experimental situation, only the LS emission angles θ are readily and accurately known; β is not known. Therefore, to define an LS rapidity $y = \text{arctanh}(\beta \cos\theta)$, y must be approximated by a pseudorapidity $\eta = \text{arctanh}(\cos\theta) = -\ln \tan(\theta/2)$. Facing this difficulty, our analysis makes use of a good approximation,¹⁴ $y \simeq \eta + \ln(p_T/m_T)$. As detailed in Appendix B, fairly large empirical correction factors, $\langle y - \eta \rangle \simeq \langle \ln(p_T/m_T) \rangle = 1.61$ and 2.71 are deduced¹⁵ for proton (deuteron or triton) fragments from the study of singly charged shower particles,¹⁶ and α fragments,^{17,18} respectively.

Thus, the angular method of Ref. 1 is extended for identifying DE events of *heavy ion beams* in nuclear emulsion with the following conditions. (i) Instead of the constraint on the second moment of the pseudorapidity distribution in Ref. 1 ("standard deviation" $= [\sum(\eta_i - \langle \eta \rangle)^2 / (n_s - 1)]^{1/2}$),³ events with charged shower particles of $\sin\theta > 0.4$ are classified as non-DE ones. This is due to the constraint condition of $\sum_i \sin\theta_i < 0.4$ of Ref. 2. (ii) The practical constraints,

$$\langle \eta_\alpha \rangle > y_b - \Delta y + 2.71 \quad \text{for } \alpha \text{ fragments}$$

and

$$\langle \eta_p \rangle > y_b - \Delta y + 1.61 \quad \text{for } p \text{ fragments} \quad (3)$$

are applied in place of Eq. (2) for the $N_h = 0$ subgroups of the interactions. [As has been mentioned above, derivation of the constants 2.71 and 1.61 in Eq. (3) is explained in detail in Appendix B.] According to Eq. (3), $\langle \eta_\alpha \rangle > 8.5, 7.4,$ and 6.1 and $\langle \eta_p \rangle > 7.4, 6.3,$ and 5.0 , respectively, for DE events of ¹⁶O ions with 200, 60, and 14.6 GeV/nucleon. These are equivalent to the average emission angle $\langle \theta_\alpha \rangle < 0.41, 1.22,$ and 4.5 mrad and $\langle \theta_p \rangle < 1.22, 3.7,$ and 13.5 mrad. On the other hand, for non-DE events, $\langle y \rangle \sim y_b/2 = 3.0, 2.4,$ and 1.7 , i.e., $\langle \theta \rangle \sim 0.13, 0.23,$ and 0.35 rad.¹⁴

Emission angles θ of singly charged shower particles and α fragments were measured, typically up to the accuracy of less than 0.1 mrad for 200-GeV/nucleon ¹⁶O, mostly with the Koristka R-4 microscopes with a magnification of $1000 \times$, with respect to heavier fragments of $Z > 2$, to the centroid of the α fragments, or to a single α track in the case of single α track events. In the rest system of their mother nucleus, especially of two-

TABLE I. The number of identified DE events.

(a) ^{16}O Mode (Eth.)	200 GeV/nucleon			60 GeV/nucleon			14.6 GeV/nucleon		
	No.	$\langle\langle\eta_p\rangle\rangle$	$\langle\langle n_\alpha\rangle\rangle$	No.	$\langle\langle\eta_p\rangle\rangle$	$\langle\langle\eta_\alpha\rangle\rangle$	No.	$\langle\langle\eta_p\rangle\rangle$	$\langle\langle\eta_\alpha\rangle\rangle$
$\alpha + ^{12}\text{C}$ (7.2)	6(37)		9.2	2		8.2	12		6.3
$p + ^{15}\text{N}$ (12.1)	25(194)	8.7		3(5)	7.5		5	5.4	
4α (14.4)	3(5)		9.4	1		8.8	1		7.4
$2d + \text{C}$ (31.8)	11(50)	7.8		-(3)			2	5.6	
$p + 2\alpha + \text{Li}$ (31.8)	1(4)	7.8	9.2	1	7.4	8.0			
$d + \alpha + ^{10}\text{B}$ (32.4)	6(13)	7.8	8.8	1	5.3	8.6	5	5.8	6.6
$^3\text{He} + \alpha + ^9\text{Be}$ (33.4)	1(1)		8.9						
$2d + 3\alpha$ (38.3)	4(19)	8.1	9.9	1	7.5	7.8	2	5.6	7.4
$2d + \alpha + \text{Be}$ (38.9)	2(5)	8.4	9.1						
$p + 2d + ^{11}\text{B}$ (47.0)	-(3)								
$p + 2d + \alpha + \text{Li}$ (55.6)	-(4)						1	5.2	6.9
$4d + 2\alpha$ (62.1)	2(11)	7.8	9.3				1	4.6	6.5
$p + 4d + \text{Li}$ (79.5)	1(1)	7.3							
$6d + \alpha$ (86.0)	1(2)	8.3		1(1)	6.6		2	5.0	
$p + \text{N} + 2\pi$ (> 320)	1	8.2							
$2d + \text{C} + 2\pi$ (> 320)	1	7.5							
$2d + 3\alpha + 2\pi$ (> 320)	2	7.8	10.0	1	6.3	7.3			
$3d + \alpha + \text{Li} + 2\pi$ (> 320)	1	7.5	8.3						
(b) ^{28}Si Mode (Eth.)	14.6 GeV/nucleon								
	No.	$\langle\langle\eta_p\rangle\rangle$	$\langle\langle\eta_\alpha\rangle\rangle$						
$^{24}\text{Mg} + \alpha$ (10.0)	4		6.8						
$^{27}\text{Al} + p$ (11.6)	15	5.8							
$^{20}\text{Ne} + 2\alpha$ (19.8)	2		6.2						
$^{23}\text{Na} + \alpha + p$ (21.7)	4	6.2	6.4						
$^{16}\text{O} + 3\alpha$ (24.0)	1		6.6						
$^{20}\text{Ne} + \text{Li} + p$ (36.7)	1	7.9							
$^{20}\text{Ne} + \alpha + 2d$ (43.2)	1	5.2	6.2						
$^{23}\text{Na} + 2d + p$ (45.6)	3	5.9							
$^{16}\text{O} + 2\alpha + 2d$ (47.9)	1	6.0	6.6						
$^{24}\text{Mg} + 2d$ (48.7)	10	6.1							
$^{14}\text{N} + 2\alpha + 3d$ (68.6)	2	5.1	6.5						
$^{16}\text{O} + \alpha + 4d$ (71.8)	1	5.7	15.6						
$3\alpha + 9p$	1	5.4	7.2						
(c) ^{32}S (Ref. 11) Mode (Eth.)	200 GeV/nucleon								
	No.								
$^{28}\text{Si} + \alpha$ (6.949)	(12)								
$^{31}\text{P} + p$ (8.865)	(150)								
$^{27}\text{Al} + \alpha + p$ (18.532)	(11)								
$^{23}\text{Na} + 2\alpha + p$ (28.625)	(2)								
$^{28}\text{Si} + 2d$ (30.797)	(52)								
$^{24}\text{Mg} + \alpha + 2d$ (40.781)	(4)								
$^{27}\text{Al} + 2d + p$ (42.383)	(8)								
$^{23}\text{Na} + \alpha + d + t$ (46.996)	(1)								
$^{19}\text{F} + 2\alpha + 2d + p$ (62.939)	(2)								
$^{24}\text{Mg} + 4d$ (64.629)	(3)								
$^{20}\text{Ne} + \alpha + 4d$ (73.984)	(1)								
$^{16}\text{O} + 2\alpha + 4d$ (78.672)	(2)								
$^{19}\text{F} + \alpha + 4d + p$ (86.787)	(1)								
$^{20}\text{Ne} + 6d$ (97.832)	(1)								
$^{14}\text{N} + 2\alpha + 5d$ (99.408)	(1)								
$^{16}\text{O} + \alpha + 6d$ (102.512)	(2)								
$^{12}\text{C} + ^7\text{Li} + \alpha + 4d + p$ (103.182)	(1)								
$^{12}\text{C} + 2\alpha + 6d$ (109.682)	(3)								
$^7\text{Li} + 4\alpha + 4d + p$ (110.457)	(1)								

body decays, heavier fragments of $Z > 2$ are usually emitted with little energy, compared with lighter partner of p or α fragments ($Z=2$), and so fly almost in the same direction as the primary projectiles do after interactions.

III. EXPERIMENTAL DATA

Tables I(a) and I(b) summarize our identified DE events of 200-, 60-, and 14.6-GeV/nucleon ^{16}O ions and 14.6-GeV/nucleon ^{28}Si ions, respectively, by applying criteria (i) and (ii) for each individual interaction. Table I (c) presents a similar summary for 200-GeV/nucleon ^{32}S ions without $\langle \eta \rangle$.¹⁹ In the first column, the modes of the decay of b^* , deduced mostly from the charge conservation and topological feature among the decay fragments, are listed and “nominal threshold energies” of the given decay modes are shown in parentheses after the modes. In each energy category of 200, 60, and 14.6 GeV/nucleon, the column lists the number of DE events identified, and in Table I(a) and I(c), the number of DE events of the corresponding mode in Ref. 11 is presented in parentheses. In the computation of the thresholds in MeV, the fragments were assumed to have zero kinetic energies in the rest frame of b^* and the adopted mode was assumed to have the least threshold among the possible modes from the given topology.

The following two columns of Table I(a) and I(b) list the averages $\langle \eta_p \rangle$ of the average of pseudorapidities of singly charged p (d or t) fragments in an event and that of α fragments $\langle \eta_\alpha \rangle$. The charges $Z > 3$ of heavy fragments of those DE events which had *two decay pions* were especially measured with the method of δ -ray counting, while all the rest of the fragments of $Z > 3$ were not identified specifically through δ -ray counting.

As shown in the Table I, the most determinative constraint on $\langle \eta_p \rangle$ for DE events is universally met by the data except for two events: An event of $d + \alpha + ^{10}\text{B}$ of 60 GeV/nucleon with $\langle \eta_p \rangle = 5.3$ (< 6.3) and another event of $4d + \alpha$ of 14.6 GeV/nucleon with $\langle \eta_p \rangle = 4.6$ (< 5.0). We took these two events as DE ones because both of them passed the $\langle \eta_\alpha \rangle$ criterion of Eq. (3). In addition to the 68 events of 200-GeV/nucleon DE events listed in Table I(a), an extra event ($2d + 3\alpha?$) had to be included in the calculation of the MFP's of DE processes which, for ^{16}O projectiles, are 1.00 ± 0.12 m (125 ± 15 mb) (Refs. 13 and 20), $2.4^{+1.6}_{-0.7}$ m (52 ± 15 mb) and 2.2 ± 0.4 m (56 ± 10 mb) for 200, 60, and 14.6 GeV/nucleon, respectively.

For ^{28}Si , the only event of the mode hard for us to identify was $3\alpha + 9p$ because all the possible decay modes of $^{28}\text{Si}^*$ violated charge and nucleon conservation. Figure 1 displays the distribution of $(\langle \eta_\alpha \rangle - y_b)$ in the upper half and that of $(\langle \eta_p \rangle - y_b)$ in the lower half of 135 $N_h = 0$ ^{28}Si events, where open squares show the 46 DE events and solid squares show the non-DE events. The average pseudorapidities $\langle \eta_\alpha \rangle$ of the DE events tend to be slightly larger than those of non-DE events, but they are all larger than the limit imposed by Eq. (3), which is shown as an arrow in the figure. As the distribution of $(\langle \eta_p \rangle - y_b)$ shows in the lower half of Fig. 1, where the arrow indicates the condition of limits imposed by Eq.

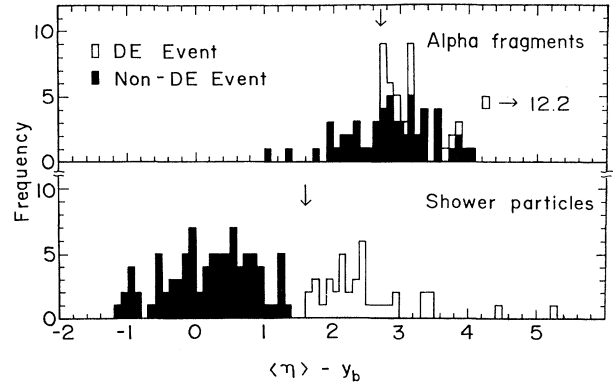


FIG. 1. Distributions of $\langle \eta_p \rangle$ and $\langle \eta_\alpha \rangle$.

(3), separation of DE and non-DE interactions of the 135 $N_h = 0$ events of 14.6-GeV/nucleon ^{28}Si is clearly feasible. Including the event of $3\alpha + 9p$, the MFP of ^{28}Si at 14.6 GeV/nucleon was obtained as 1.09 ± 0.13 m (114 ± 14 mb).

The “apparent” MFP versus the primary energy E_b is plotted in Fig. 2. Since detection efficiency is not assessed and modes which include decay neutrons or neutral pions are not included, the “apparent” MFP's should be taken as upper-limit values.

Figure 3 shows the proportion of decay modes of $^{16}\text{O}^*$ among three intervals, 0–30, 30–60, and 60–90 MeV of the “nominal threshold energy” for all the DE events (excluding those with two pions) in Table I using solid circles for 14.6 GeV/nucleon, shaded ones for 60 GeV/nucleon and open circles for 200 GeV/nucleon. No strong dependence of the proportion on E_b is noticed in Fig. 3. In the range of $E_b = 14.6$ –200 GeV/nucleon for ^{16}O , the dependence on the nominal threshold energy seems to be approximately the same for the various breakup channels.²¹ The solid line histogram is our combined result for ^{16}O ions and displays the *rough* trend of $\exp\{a\Delta m + b\}$ with $a = -0.025 \pm 0.005$ ($\chi^2/N_{\text{DF}} = 7/1$), while the dashed-line histogram represents the recent combined data of DE events of Ref. 11 in Table I with $a = -0.036 \pm 0.003$ ($\chi^2/N_{\text{DF}} = 16/1$). Figure 4 displays

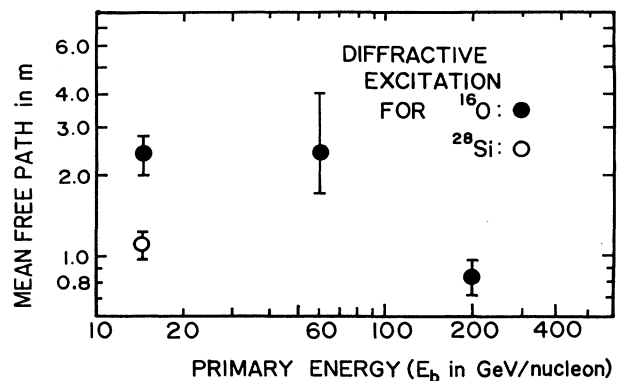


FIG. 2. The “apparent” DE MFP in m vs E_b .

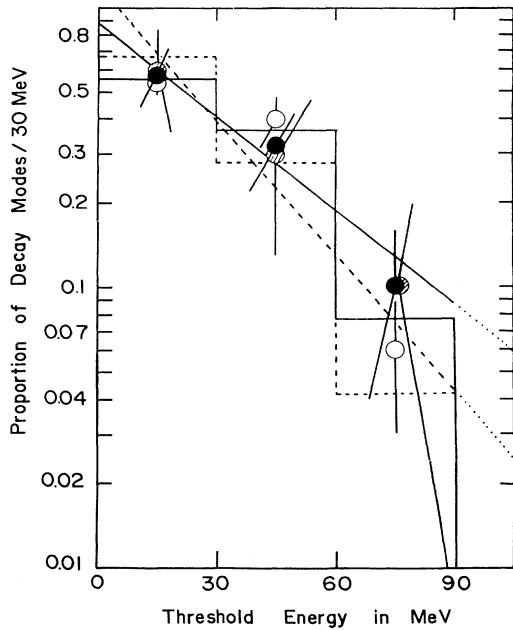


FIG. 3. Proportion of decay modes according to the “nominal threshold energy” for $^{16}\text{O}^*$. Solid circle, shaded one, and open one, respectively, for 14.6, 60, and 200 GeV/nucleon.

proportion of occurrence of decay modes in terms of “nominal threshold energy” for the intervals 0–30, 30–60, and 60–90 MeV by open circles for the 14.6-GeV/nucleon ^{28}Si data with the rough trend of $\exp(a\Delta m + b)$ with $a = -0.025 \pm 0.008$ ($\chi^2/N_{\text{DF}} = 2/1$). Included in the same plot are the proportion of decay modes for the combined data of 14.6-, 60-, and 200-GeV/nucleon ^{16}O from our data plus the massive data of

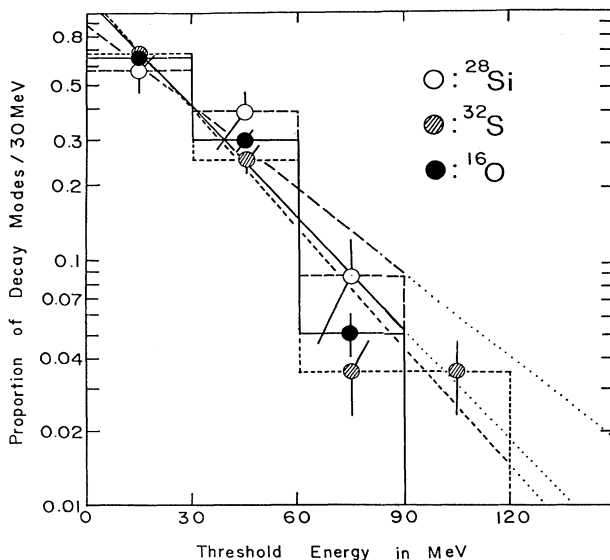


FIG. 4. Proportion of decay modes according to the “nominal threshold energy.”

Ref. 11 with $a = -0.034 \pm 0.003$ ($\chi^2/N_{\text{DF}} = 21/1$) as shown by the solid circles and for the same authors, data of 200-GeV/nucleon ^{32}S for the four intervals 0–30, 30–60, 60–90, and 90–120 MeV with $a = -0.036 \pm 0.003$ ($\chi^2/N_{\text{DF}} = 7/2$) as shown by the shaded circles.

IV. DISCUSSIONS AND CONCLUSIONS

In the present experiment by use of a new powerful angular method for identifying DE events of projectile heavy ions in nuclear emulsion, *firstly*, preliminary trends of high-energy augmentation of DE process may be concluded. Due to the factor of $\sinh y_b$ ($\simeq \gamma_b$ for the large Lorentz factor γ_b), Eq. (1) shows that, even with a longitudinal momentum transfer of as small as ~ 0.03 GeV/c, a few excited states of high mass m_{b^*} can be reached from the ground state of a projectile beam nucleus, as the primary rapidity y_b (i.e., E_b) becomes large (see Appendix A).

Secondly, as shown in Figs. 3 and 4, almost all the possible modes of decay, up to several hundreds of MeV/c² of Δm are found to occur independently of the kind of incident projectile heavy ion b and its incident energy E_b and with exponentially decreasing trend with almost the same exponential index $a = (-0.2)(-0.3)$,²² i.e., the higher the mass of b^* is, the harder it becomes to produce. Further, the fact that the proportions of various breakup channels of b^* (except those with pion production) seem to have no dependence on E_b for the soft-breakup processes reminds us that, because of Eq. (1) as well as the above considerations, the distribution of Δm reflects that of the longitudinal momentum transfer to the target nucleus q_L [$\simeq (m_{b^*}^2 - m_b^2)/2E_b \simeq (m_{b^*} + m_b)\Delta m/2m_b\gamma_b \simeq \Delta m/\gamma_b$]. Since the distribution of $\gamma_b q_L \simeq \Delta m$ is independent of γ_b , the DE process requires less q_L for larger γ_b .

Thirdly, as seen from Figs. 3 and 4, at least 60–70% of DE events are those with the removal of a proton or an α fragment from the projectile ($\Delta Z \leq 2$), which supplements the extensive information obtained from other experiments involving fragmentation or DE processes.⁹

In this context, there have been past investigations of keen interest about high-energy μ -emulsion interactions,^{23–25} since the electromagnetic field of a muon will induce soft breakup of C, N, O, Ag, Br nuclei in nuclear emulsion which must be the inverse of the projectile DE (the “target” DE) of the present experiment in the anti-laboratory system (ALS). And about 80% of them must be in the form³ of $(1+1)$ with emission of an α or p with $\theta \sim 90^\circ$ in th LS. Reference 25 clearly gives the impression of abundant and enhanced production of pions with 150-GeV μ^+ jets,²⁵ which may correspond to the formation of a Δ by the “target” DE process in the ALS and coincides with our present experiment as opposed to 5 GeV/c (Ref. 23), 10.1- and 15.8-GeV μ jets.²⁴

Also, many semiclassical calculations based on the Weizsacker-Williams method for virtual photons²⁶ have been done to obtain the cross sections of electromagnetic dissociations (see, for example, Refs. 9 and 27). But to our knowledge, no serious theoretical calculations to at-

tack the DE processes fully have been done (see Appendix A).²⁸

Fourthly, the majority of DE events of soft splitting of incident heavy ions in our data may be attributed to the Coulomb interactions as well as to “grazing” nuclear collisions. Sixty-four events, out of a total of the 69 events of 200-GeV/nucleon ^{16}O (68 events, listed in Table I, plus one extra event), for example, belong to this category. On the other hand, the remaining five *high-energy* DE events of 200 GeV/nucleon (and one DE event of 60 GeV/nucleon and none in the data of 14.6-GeV/nucleon events) with two decay pion, which were not particularly investigated in Refs. 9–11, should be attributed to the onset of some “new” contributions. An indication of a drastic increase of DE events with the fragmentation plus the emission of an additional two pions from $E_b = 14.6$ GeV/nucleon to 200 GeV/nucleon coincides with that of DE events from 30 to 400-GeV protons¹ where a Δ resonance may be involved primarily (also Δ production in the LS by muons as mentioned above, see Appendix A).

The implication of the present experiment might be summarized well by use of the uncertainty relation in both the transverse and longitudinal directions. When the interacting two nuclei are viewed as *two whole entities* having the *largest* dimensions of their hierarchy among our three points of view for looking at a nucleus—(a) as a whole entity in decay and excitation, neglecting the size of a nucleon, (b) as an aggregate of A_b and A_t nucleons individually, and (c) as an aggregate of quarks and gluons—their “interaction” radius must be the order of $R \simeq (A_b^{1/3} + A_t^{1/3})/m_\pi$ so that

$$q_T R \sim 1 \quad (4)$$

from the diffractive condition, and, since the distribution of $\Delta m \simeq \gamma_b q_L$ seems almost independent of the incident energy E_b and the mass of the projectile A_b ,

$$\gamma_b q_L R' \sim 1, \quad (5)$$

where $R' \simeq R/\gamma_b$, the Lorentz-contracted size of the target nucleus as seen by the incident heavy ion, which guarantees $q_L R \sim 1$. This condition has been the starting point of defining DE process and has been retrieved as the concluding one from the data of Δm distribution. The next *smaller* ladder of hierarchy (b) of looking at A_b and A_t nucleons individually is to take them as two aggregates of $(A_b + A_t)$ nucleons, interacting individually. In these interactions between a nucleon and another nucleon,

$$q_{TN} R_N \sim 1, \quad (4')$$

where the size of a nucleon $R_N \sim 1/m_\pi$, and

$$\gamma_b q_{LN} R'_N \sim 1, \quad (5')$$

indicating $\Delta m_{bN} \simeq \gamma_b q_{LN}$ which is an order of magnitude larger than values involved in two collisions of two whole nuclei in the first ladder of the hierarchy (a). The fact that the MFP (of ~ 0.1 m for 200-GeV nucleon ^{16}O) of DE interactions with pion production is the same order as that (of ~ 0.2 m for 200 GeV proton) of (0+3) events

in the high-energy proton-emulsion collisions¹ convinces us of this point. The excitation and decay of the baryon multiplets involve hundreds of MeV. Thus, we may have two kinds of soft processes of DE interactions, with and without pion production, which are distinctively different from the third *smallest* ladder of hierarchy (c)—looking at an interaction of two nuclei as quark-quark interactions with “multiple” production of medium and high p_T —whose aspects and properties were exploited preliminarily by our group.²⁹

For one direct application of the DE process, we may be able to explain the puzzle of the cosmic ray physics: The Centrauro events observed in emulsion chambers exposed to cosmic rays³⁰ are very high-energy events characterized by a very large multiplicity of *hadrons* and a multiplicity of electromagnetic showers that is consistent with zero.³¹ Hadron parts would be observed decay fragments produced in DE interactions of heavy primary cosmic rays ($Z > 1$) without producing any *pion* components, among which π^0 s give rise to electromagnetic showers from $\pi^0 \rightarrow 2\gamma$.

In view of recent advances in accelerating heavy ions at BNL AGS, CERN SPS and in the future at the BNL RHIC, the aspect of high-energy DE interactions will provide an opportunity for study of clean breakups of high-mass excited states of various beam nuclei of the “LS” lifetimes $\simeq 10^{-21}$ sec or longer (see Appendix A). Further, as far as kinematics are concerned and *contrary* to the common belief that “deconfinement” will occur only in central collision, the high-mass state of $m_{b^*} > 10m_b$, especially because of its long lifetime in order to attain equilibrium state in the whole system of nucleon of the same size with the “higher” energy density, will be able to be produced copiously in the CERN SPS and BNL RHIC colliders for the investigation of the “deconfinement phase transition” of nuclei through the DE process.⁵

ACKNOWLEDGMENTS

The National Science Foundation supported this work partially under Grant No. PHY-8604315 as well as the Korea Science and Engineering Foundation; Non-Directed Research Fund, Korea Research Foundation; and the Basic Science Research Institute Program, Ministry of Education, Republic of Korea. We thank the members of the KLM Collaboration for providing emulsion plates exposed to oxygen and silicon beams at BNL and CERN as well as for making available the analysis on some of the KLM data. The processing team of FNAL E 653 at Fermilab is also appreciated for their processing of the two stacks we have used in the present experiment of ^{28}Si , and we thank Professor R. J. Wilkes of Department of Physics, University of Washington for their exposure at BNL.

APPENDIX A: DERIVATION OF EQ. (1) AND THE DIFFRACTIVE EXCITATION (DE) PROCESS

Essentially with the same argument as in Ref. 1, Eq. (1) is derived in the following. For an incident beam particle

with LS primary energy $E_b = m_b \cosh y_b$ in the quasi-two-body (DE) interaction

$$b + A_t \rightarrow b^* + A_t, \quad (\text{A1})$$

where A_t stands for the constituent target nucleus of mass number A_t in nuclear emulsion, the LS energy of the high-mass state b^* becomes $E_{b^*} = (m_{b^*}^2 + q_T^2)^{1/2} \cosh y_{b^*} \simeq m_{b^*} \cosh y_{b^*}$. Because of the “diffractive” condition (or equivalently, the uncertainty relation) of the process (A1),

$$q_T R \simeq 1, \quad (\text{A2})$$

where q_T is the transverse momentum transfer to the largest nucleus and R , the “interaction” nuclear radius obtained by looking at the incident and target nuclei as one entity. Thus, we may assume $R \sim (A_b^{1/3} + A_t^{1/3})/m_\pi$ ($1/m_\pi \simeq 1.41$ fm, numerically) and $q_T^2/2A_t m_N < 0.001$ GeV, which guarantees the last step of the approximation involved in E_{b^*} in the above. Further, the condition^{6,7} relating the longitudinal momentum transfer q_L to the target and R ,

$$q_L R \ll 1 \quad (\text{A3})$$

amounts to “virtuality (or coherence)” with respect to the individual constituents of b .

Thus, from the energy conservation equation for process (A1), we have

$$E_b + A_t m_N = E_{b^*} + (A_t m_N + T_A) \quad (\text{A4})$$

which is equivalent to

$$m_b \cosh y_b \simeq m_{b^*} \cosh y_{b^*} \quad (\text{A5})$$

to a good approximation in the DE process since the nuclear recoil kinetic energy plus the energy transferred to the internal restructuring of b^* , if there is any, $T_A = q^2/2A_t m_N < 0.001$ GeV can be neglected due to Eqs. (A2) and (A3).

For interactions of $E_b > 10$ GeV/nucleon (or 10 GeV for a hadron), Eq. (A5) can be well approximated as $m_b (\exp y_b)/2 \simeq m_{b^*} (\exp y_{b^*})/2$, indicating

$$\Delta y = y_b - y_{b^*} \simeq \ln(m_{b^*}/m_b). \quad (\text{A6})$$

Now, secondly from the conservation of longitudinal momenta for the process (A1), we have

$$p_b = p_{b^*} + q_L \quad (\text{A7})$$

which corresponds to

$$\begin{aligned} m_b \sinh y_b &= (m_{b^*}^2 + q_T^2)^{1/2} \sinh y_{b^*} + q_L \\ &\simeq m_{b^*} \sinh y_{b^*} + q_L. \end{aligned} \quad (\text{A8})$$

Multiply both sides of Eqs. (A4) and (A8) by $\cosh y_b$ and $\sinh y_b$, respectively, and subtracting the two resulting equations, we have

$$m_b + q_L \sinh y_b \simeq m_{b^*} \cosh(-\Delta y). \quad (\text{A9})$$

Also multiplying both sides of these same equations by $\sinh y_b \cosh y_b$ and subtracting the two resulting equations, we have

$$q_L \cosh y_b \simeq m_b \sinh(\Delta y). \quad (\text{A10})$$

After squaring Eqs. (A9) and (A10), we add the two resulting equations to obtain Eq. (1)

$$m_{b^*} \simeq m_b (1 - q_L^2/m_b^2 + 2q_L \sinh y_b/m_b)^{1/2}$$

in the text.

Now to understand the mechanism of how large mass m_{b^*} can be created from the projectile of mass m_b without transferring large energy (in fact, little energy) to the target nucleus, our picture of these DE processes at high-energy attribute it to the intrinsic “wave” nature of the incident and the diffracted beam. The diffractive condition of Eq. (A1), $q_T R \simeq 1$, implies the deviation angle of $\theta_{b^*} (\neq 0)$ for b^* , since $q_T = q \sin \theta_{b^*}$.

From Eq. (A5), where $y_{b^*} = \tanh^{-1}(\beta_{b^*} \cos \theta_{b^*})$ (Ref. 14), $\cos \theta_{b^*} < 1$ (and $\beta_{b^*} \simeq \beta_b \sim 1$) assures $y_{b^*} < y_b$ ($\Delta y \simeq y_b - y_{b^*} = \ln(m_{b^*}/m_b) > 0$) and consequently $m_{b^*} > m_b$ from the approximate equality of Eq. (A5). Thus, we insist that the increase of m_{b^*} (as much as up to $m_{b^*} \simeq 10m_b$ easily at RHIC energy) comes from the intrinsic wave nature due to the opaque or semiopaque disk represented by the target nucleus. In other words, the relativistic effect played the cardinal role of increasing the rest mass of projectile nucleus. Thus, the large mass excitation with the small momentum transfer (or energy transfer) to the target, i.e., Δm (in GeV/ c^2) $\gg \Delta E$ (in GeV) of our picture, may imply that the prevailing calculation of electromagnetic dissociation may be at fault especially at large $\sinh y_b (\simeq y_b)$, since the authors in Ref.

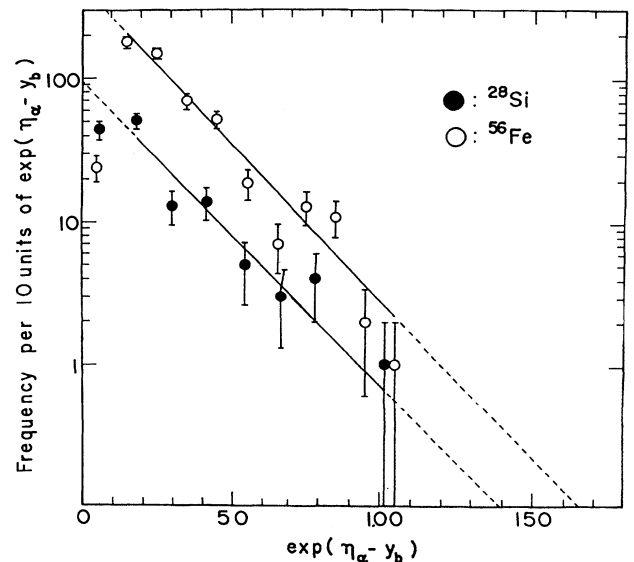


FIG. 5. Frequencies of occurrence of α fragments vs $\exp(\eta_\alpha - y_b)$ in nuclear emulsion.

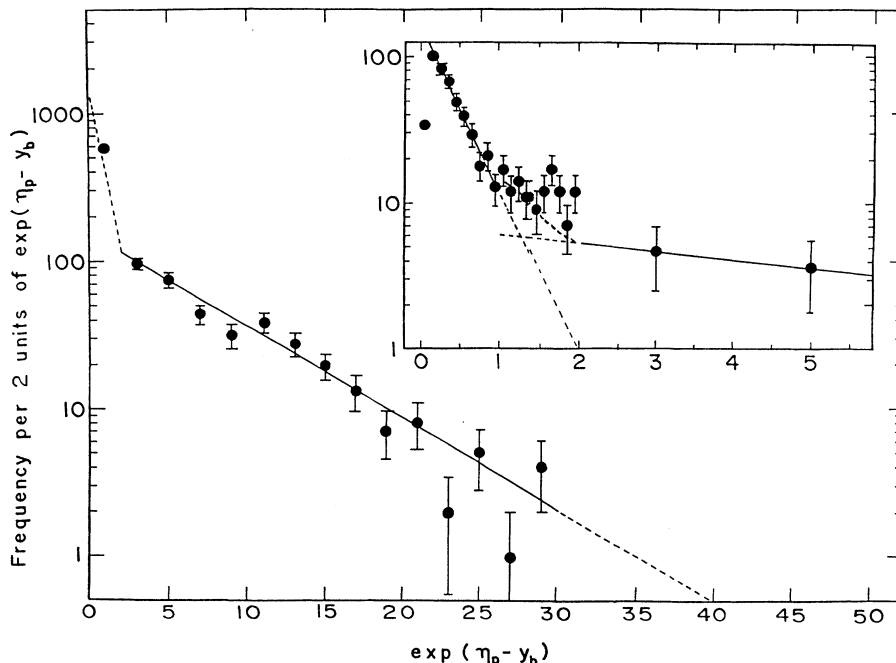


FIG. 6. Frequencies of occurrence of singly charged secondaries of 14.6-GeV/nucleon ^{28}Si in nuclear emulsion.

9 assume Δm (in GeV/c^2) $\sim \Delta E$ (in GeV) universally. There are two consequences which can be checked experimentally: The first is the high-energy augmentation of DE process because, for us, it would require less q_L and the absorption of the lower-energy ($E_\gamma < 1$ MeV) part of the virtual-photon spectrum ($\propto \ln \gamma_b Z_T^2 / E_\gamma$) than for the authors of Ref. 9 ($E_\gamma \approx 10$ – 30 MeV), even in using the Weizacker-Williams method²⁶ for the electromagnetic contribution of the DE process (the predominant dependences of $A_T^{1/3}$ and Z_T have been well investigated by Barrette *et al.* in Ref. 9). In this respect, our observation of increase in DE interactions *with pions* for large γ_b supports our view, since they involve $E_\gamma > 280$ MeV and cannot be produced directly by the giant dipole resonance of $E_\gamma \approx 10$ – 30 MeV. The preliminary evidence of abundant production of Δ for high-energy μ (as it should) in nuclear emulsion,^{23–25} will also support our view since Δm ($\approx 200 \text{ GeV}/c^2$) $> \sim 20$ MeV, which should be the energy that the predominant role of giant dipole resonance is solely assumed. For the μ , it will be far more important to investigate this phenomena further, since the DE processes is induced due to purely electromagnetic field. This is more so since $\Delta m \approx \gamma_b q_L$ remains independent of E_b from our observation.

The second consequence may be for us to prove the existence of b^* states with their long LS lifetimes $\approx 10^{-21}$ sec in the continuum, which is partially proven by our data indicating the universal validity of Eq. (3). Since our observed lifetime is $\gamma_b \tau \approx 10^{-21}$ sec, more states with the intrinsic short lifetime τ will be allowed to leave and to decay outside the target, where the very DE interactions take place, as γ_b increase. For example, in order to

create Δ on the mass shell, γ_b must be fairly large, which is the alternative way of explaining the DE process.

APPENDIX B: THE RELATION BETWEEN LS RAPIDITY y AND PSEUDORAPIDITY η

There has been a good approximate relation between the LS rapidity y and the pseudorapidity η , $y \approx \eta + \ln(p_T/m_T)$.¹⁴ The parameter $u = p_T/m_T$ [$= \exp(y - \eta)$] can also be expressed as $u = \bar{\gamma}_b \bar{\beta}_b \sin \theta \approx \bar{\beta}_T$ for p or α fragments in the rest system of incident heavy ions (the antilaboratory system, ALS) and, since $\bar{\beta} \ll 1$, $\bar{\gamma} \sim 1$ for p or α fragments.²¹ As shown for 2,188 α fragments produced in Fe-C and Fe-Pb collisions at 1.88 GeV/nucleon,¹⁷ the inclusive distribution of $\bar{\beta}_T \approx u$ may be well expressed by

$$dN = \exp(c + \kappa/\bar{\beta}_T) d(1/\bar{\beta}_T) \quad (\text{B1})$$

with $\kappa = 0.0457 \pm 0.0011$. On the other hand, the relation

$$\exp(\eta - y_b) = \exp[(y - y_b) - (y - \eta)]$$

becomes

$$\exp(\eta - y_b) \approx 1/u \approx 1/\bar{\beta}_T,$$

since $\langle y - y_b \rangle = \langle \bar{y} \rangle = 0$ on the average, individually for each interaction in the ALS. Thus, in terms of $\exp(\eta - y_b)$, Figure 5 shows frequencies of occurrence of the α fragments, produced in 135 $N_h = 0$ interactions of 14.6-GeV/nucleon ^{28}Si nuclei in nuclear emulsion,¹⁶ (solid circles), and 344 interactions of 1.88-GeV/nucleon

^{56}Fe nuclei in nuclear emulsion¹⁸ (open circles), which gave, respectively, $\kappa=0.050\pm 0.006$ and 0.048 ± 0.003 ($\chi^2/N_{\text{DF}}=9/5$ and $24/8$ for the fits). The combined value of $\kappa=0.046\pm 0.0010$ from the above three data at tests the “limiting fragmentation.”^{15,32}

By combining Eqs. (3) and (6) of Ref. 17, the median angle $\theta^{1/2}$ is obtained as $(\cot\theta)^{1/2}=\ln(2\gamma_b\beta_b/\kappa)$, which give $\theta^{1/2}=\text{arccot}[(\cot\theta)^{1/2}]$ with plausible assumption of $\gamma\beta\approx\gamma_b\beta_b$. Thus we obtain $\langle \ln u \rangle = 2.71$.

As for singly charged shower particles, there are roughly two kinds of produced secondaries: p (possibly d or t) fragments and pions (or kaons) of “pionization.” In

view of our success of finding a law of emission, for α fragments, Eq. (B1), shown in Fig. 5 and in Ref. 16, the differential frequency of occurrence of singly charged shower particles, produced in 135 14.6-GeV/nucleon ^{28}Si nuclei in nuclear emulsion,¹⁶ is shown in Fig. 6 in terms of $\exp(\eta_p - y_b)$. The general trends can be well fitted with two linear regression functions in the semilog plots, resulting in the best fitted values of $\kappa = -2.5\pm 0.2$ [$\chi^2/N_{\text{DF}}=2/7$ for the interval $0.1 < \exp(\eta_p - y_b) < 1$] and $\kappa = -0.138\pm 0.008$ [$\chi^2/N_{\text{DF}}=13/14$ for the interval $2 < \exp(\eta_p - y_b) < 34$]. From the latter value of κ , we obtained, as in the above for α fragments, $\langle \ln u \rangle = 1.61$.

¹C. O. Kim, K. P. Hong, and J. N. Park, *J. Korean Phys. Soc.* (Seoul) **13**, 90 (1980). Unfortunately, there has been an error of a factor of 2 in Eq. (12) of the paper, which is equivalent to Eq. (1) of the present paper. Nevertheless, instead of taking $q_{L\text{max}}=0.06$ GeV/c, the paper took $q_{L\text{max}}=0.03$ GeV/c, which compensated for the factor of 2 and rendered all the final deductions and results of the paper valid.

²S. A. Azimov *et al.*, *Dokl. Akad. Nauk SSSR* **192**, 1241 (1970) [*Sov. Phys. Dokl.* **15**, 569 (1970)]; G. B. Zhdanov, M. I. Tret'yakova and M. M. Chearnyavskii, *Zh. Eksp. Teor. Fiz.* **55**, 170 (1968) [*Sov. Phys. JETP* **28**, 91 (1969)]; S. A. Azimov *et al.*, *Dokl. Akad. Nauk SSSR* **212**, 1323 (1973) [*Sov. Phys. Dokl.* **18**, 662 (1974)]; M. G. Antonova *et al.*, *Phys. Lett.* **39B**, 285 (1972); S. A. Azimov *et al.*, *Dokl. Akad. Nauk SSSR* **218**, 807 (1974) [*Sov. Phys. Dokl.* **19**, 669 (1975)]; P. J. Jain *et al.*, *Lett. Nuovo Cimento* **9**, 113 (1973); S. Konishi *et al.*, *Phys. Rev. D* **13**, 1826 (1976); E. G. Boos *et al.*, *Nucl. Phys.* **B137**, 37 (1978); Alma-Ata-Gatchina-Moscow-Tashkent Collaboration, *Yad. Fiz.* **30**, 407 (1979) [*Sov. J. Nucl. Phys.* **30**, 210 (1979)].

³According to the Bristol convention, a “star” found in nuclear emulsion is classified as $(N_h + n_s)$, where N_h is the number of grey particles or heavy prongs of LS velocity $\beta < 0.7$ and n_s that of charged shower particles $\beta > 0.7$. Thus, these interactions are classified as $N_h = 0$. If $N_h > 8$, we can be certain that the target nucleus is one of the heaviest constituent nuclei (Ag, Br) of nuclear emulsion.

⁴L. Van Hove, *Usp. Fiz. Nauk.* **124**, 509 (1978) [*Sov. Phys. Usp.* **21**, 252 (1978)].

⁵M. A. Faessler, *Nucl. Phys.* **A447**, 455c (1985); K. Goulianos, *Nucl. Phys. B (Proc. Suppl.)* **12**, 110 (1990).

⁶E. L. Feinberg and I. Pomerancuk, *Nuovo Cimento Suppl.* **3**, 652 (1956).

⁷M. L. Good and W. D. Walker, *Phys. Rev.* **120**, 1855 (1960).

⁸F. Ajzenberg-Selove, *Nucl. Phys.* **A375**, 1 (1982). Some of the narrow level structures of $^{16}\text{O}^*$ are seen here.

⁹J. C. Hill *et al.*, *Phys. Rev. Lett.* **60**, 999 (1988); P. B. Price, R. Guoxiao, and W. T. Williams, *Phys. Rev. Lett.* **61**, 2193 (1988); J. C. Hill, *Phys. Rev. C* **39**, 524 (1989); J. R. Beene *et al.*, *ibid.* **41**, 920 (1980); J. Barrette *et al.*, *ibid.* **41**, 1512 (1990); G. Singh, K. Sengupta, and P. J. Jain, *ibid.* **41**, 999 (1990), and references quoted therein.

¹⁰N. Ardito *et al.*, *Europhys. Lett.* **6**, 131 (1988).

¹¹A talk given by A. C. Breslin of the group of Ref. 10 at the Japan-US Seminar on Present and Future of Experimental Particle Physics by Hybrid Emulsion-Electronic Detectors, Nagoya, Japan, 1989 (unpublished).

¹²For BR-2 emulsion ($\rho=3.92$ g/cm³), the mean-free path

$\lambda(\text{g/cm}^2)=\bar{A}/[6.04\times 10^{-4}\sigma(\text{mb})]$ with $\bar{A}=29.5$. See M. P. Kertzman, Ph.D. thesis, University of Minnesota, 1987. The same formula is applied also to Fuji ET-7B emulsion.

¹³L. M. Barbier *et al.*, *Phys. Rev. Lett.* **60**, 405 (1988); H. von Gersdorff *et al.*, *Phys. Rev. C* **39**, 1385 (1989); L. M. Barbier *et al.*, *Nucl. Phys.* **A498**, 535c (1989).

¹⁴C. O. Kim, *Phys. Rev.* **158**, 1261 (1967); *Phys. Rev. D* **31**, 513 (1985); A. Dar, I. Otterlund, and E. Stenlund, *ibid.* **20**, 2349 (1979).

¹⁵I. T. Lim, Ph.D. thesis, Korea University, 1988; S. D. Chang *et al.*, *J. Korean Phys. Soc.* (Seoul) **23**, 116 (1990).

¹⁶K. Y. Kim, M. S. thesis, Korea University, 1988; C. O. Kim *et al.*, *New Physics* [*Korean Phys. Soc.* (Seoul)] **30**, 111 (1990).

¹⁷C. O. Kim *et al.*, *Phys. Rev. C* **32**, 1454 (1985).

¹⁸D. G. Koo, Ph.D. thesis, Korea University, 1987.

¹⁹Selection of DE events in Ref. 11 was carried out not exactly by our present method of applying the criteria of Eq. (3), and, nevertheless, the same trends of the Δm distribution as ours are shown in Fig. 4. As stated in the text, identification of DE events can be routinely achieved by inspection under the microscope only.

²⁰In m , our values of MFP for the various channels coincide largely with those of Ref. 10, as seen in Table I. However, there is no available data from experiments other than those in nuclear emulsion that can be compared directly with our results. To an order of magnitude, our results match favorably also with $\sigma(^{16}\text{O-Al}$ at 200 GeV/nucleon) of the counter experiments by P. D. Barnes *et al.*, *Phys. Lett. B* **206**, 146 (1988).

²¹There is one exception seen in Table I(a), due probably to the detection efficiency. The ratio of frequency of the mode $p + ^{15}\text{N}$ to that of $\alpha + ^{12}\text{C}$ is 4~5 at 200 GeV/nucleon but only 0.4 at 14.6 GeV/nucleon. The detection efficiency of the latter mode should be ~100%, while the usage of $125\times$ magnification at 14.6 GeV/nucleon might have hindered full detection of the minimum-ionizing particle of p for the former mode. In addition to the fact that their emission angles θ_p at 14.6 GeV/nucleon are fairly large, which makes their detection harder. Nevertheless, because we used $750\times$ magnification, the same is not true for 14.6-GeV/nucleon ^{28}Si , as seen from Table I(b). The ratio of the frequency of the mode $p + ^{31}\text{P}$ to that of $\alpha + ^{28}\text{Si}$ in Table I(c) is more than 10. This is definitely proven by Barrette *et al.* (Ref. 9).

²²Experimental estimates about small kinetic energies of p (d or t) and α fragments in the rest frame of the incident ^{16}O ions have been made by D. E. Greiner *et al.* [*Phys. Rev. Lett.* **35**, 152 (1975)] at 2.1 GeV/nucleon: $T_p \approx 5$ MeV and $T_\alpha \approx 2.5$

- MeV. Adding these kinetic energies to the estimates of the “nominal threshold energies” does not seem to change the above trend very much.
- ²³P. J. MacNulty and P. L. Jain, *Phys. Rev.* **183**, 1160 (1969).
- ²⁴P. L. Jain and A. Stern, *Phys. Rev. Lett.* **26**, 980 (1971).
- ²⁵P. L. Jain and K. Sengupta, *Z. Phys. C* **36**, 45 (1987).
- ²⁶J. D. Jackson, *Classical Electrodynamics*, 2nd Ed. (Wiley, New York, 1975), p. 719.
- ²⁷C. Brechtmann, W. Heinrich, and E. V. Benton, *Phys. Rev. C* **39**, 2222 (1989).
- ²⁸C. J. Benesh, B. C. Cook, and J. P. Vary, *Phys. Rev. C* **40**, 1198 (1989).
- ²⁹C. O. Kim and Eun-Suk Seo, *J. Korean Phys. Soc. (Seoul)* **20**, 292 (1987).
- ³⁰Brazil-Japan Collaboration, Fujimoto *et al.*, *Proceedings of the 13th International Cosmic Ray Conference, Denver, 1973* (University of Denver) Denver, CO, 1973), Vol. 3, p. 2227; *ibid.* Vol. 4, p. 2671.
- ³¹C. Albajar *et al.*, *Nucl. Phys.* **B335**, 261 (1990).
- ³²J. Benecke *et al.*, *Phys. Rev.* **188**, 2159 (1969); T. T. Chou and C. N. Yang, *Phys. Rev. Lett.* **25**, 1072 (1970).